Article

Cite This: *Biomacromolecules* XXXX, XXX, XXX−XXX

pubs.acs.org/Biomac

Cyclam-Modified PEI for Combined VEGF siRNA Silencing and CXCR4 Inhibition To Treat Metastatic Breast Cancer

Yiwen Zhou,[†,§] Fei Yu,[‡,§] Feiran Zhang,[†] Gang Chen,[†] Kaikai Wang,[†] Minjie Sun,[†] Jing Li,[‡] and David Oupický*[,†,‡]

[†]State Key Laboratory of Natural Medicines, Department of Pharmaceutics, China Pharmaceutical University, Nanjing, 210009, China

[‡]Center for Drug Delivery and Nanomedicine, Department of Pharmaceutical Sciences, University of Nebraska Medical Center, Omaha Nebraska 68198, United States

ABSTRACT: Chemokine receptor CXCR4 plays an important role in cancer cell invasion and metastasis. Recent findings suggest that anti-VEGF therapies upregulate CXCR4 expression, which contributes to resistance to antiangiogenic therapies. Here, we report the development of novel derivatives of polyethylenimine (PEI) that effectively inhibit CXCR4 while delivering anti-VEGF siRNA. PEI was alkylated with different amounts of a CXCR4-binding cyclam derivative to prepare PEI-C. Modification with the cyclam derivatives resulted in a considerable decrease in cytotoxicity when compared with unmodified PEI. All the PEI-C showed significant CXCR4 antagonism and the ability to inhibit cancer cell invasion. Polyplexes of PEI-C prepared with siVEGF showed effective silencing of the VEGF expression in vitro. In vivo testing in a syngeneic breast cancer model showed promising antitumor and antimetastatic activity of the PEI-C/siVEGF polyplexes. Our data demonstrate the feasibility of using PEI-C as a carrier for simultaneous VEGF silencing and CXCR4 inhibition for enhanced antiangiogenic cancer therapies.

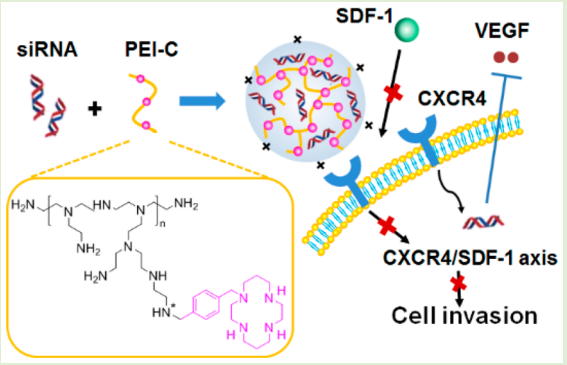

1. INTRODUCTION

Vascular endothelial growth factor (VEGF) is one of the most critical regulators of tumor-induced angiogenesis, which facilitates tumor growth and survival. In breast cancer, VEGF overexpression markedly increases intratumoral lymphangiogenesis, resulting in significantly enhanced metastasis to regional lymph nodes and to the lung.[1] Antiangiogenic therapy with monoclonal antibodies has been successfully used clinically in the treatment of various cancers. Gene silencing with siRNA has been used in preclinical studies as an alternative approach to VEGF inhibition by antibodies and has been reported to control tumor growth, inhibit metastasis, and prolong survival.[2,3] Despite the clear benefits of VEGF inhibition, the improvement of survival has often been modest. Recent reports suggested that many anti-VEGF therapies upregulate expression of the CXCR4 chemokine receptor as well as the expression of its ligand stromal derived factor-1 (SDF-1).[4,5] Available evidence shows that VEGF and CXCR4 expression are highly correlated and might synergistically promote lymphatic metastasis in various cancers.[6−9]

Chemokines and chemokine receptors form a complex network involved in a variety of homeostatic and pathological activities. Among the family of over 40 chemokines and their receptors, SDF-1 (also known as CXCL12) along with its receptor CXCR4 are highlighted in regulating tumor metastasis, proliferation, survival, and angiogenesis in various types of metastatic cancers including breast cancer.[10−12] Metastatic breast cancer has a poor prognosis as currently there is no effective treatment for patients diagnosed with this disease.[13] Recent studies have suggested that breast cancers overexpressing CXCR4 have a tendency to metastasize to distant sites where SDF-1 levels are high, including lung, liver, lymph nodes, and bones.[14] CXCR4 regulates the chemotactic function via activation of several intracellular signaling transduction pathways, including PI3K, MAPK, and Erk1/2 upon binding and interaction of the receptor and the ligand.[15] Blockade of such interactions using CXCR4 antagonists like AMD3100 (Plerixafor) have shown significant reduction of cancer metastasis.[16,17]

RNA interference (RNAi) has emerged as a potential tool for treating various genetic and acquired diseases such as cancer.[18−21] Targeted delivery of siRNA to cancer cells is a complicated and challenging process and the lack of efficient and safe delivery platforms remains a major hurdle for successful clinical application of RNAi.[22] Cationic polymers have been extensively explored for delivering siRNA because they are able to efficiently complex siRNA and protect it from degradation and facilitate siRNA transport across cellular membranes.[23,24] Polyethylenimine (PEI) is one of the most studied nonviral nucleic acid carriers due to its high transfection

Received: October 16, 2017
Revised: January 3, 2018

DOI: 10.1021/acs.biomac.7b01487
Biomacromolecules XXXX, XXX, XXX−XXX

efficacy both in vitro and in vivo.[25,26] PEI is known to efficiently facilitate endosomal escape of the polyplexes, in part due to its high charge density which contributes to its membrane-active properties. However, such high charge density also leads to high cytotoxicity, which has been a major concern for PEI that limits its development. Multiple approaches have been advanced to overcome the toxicity issue, including changing molecular weight and architecture of the polymer,[27,28] modification of amines with hydrophobic moieties,[29] introduction of biodegradable bonds to the PEI backbone,[30−32] and combining PEI with lipid components to form hybrid polycation liposomes.[33,34] We have previously developed a series of polycationic CXCR4 antagonists that can not only limit cancer metastasis but also deliver therapeutic nucleic acids like siRNA.[35−38] In this study, we present a novel strategy to modify PEI with a cyclam-based CXCR4 antagonist. Toxicity, CXCR4 antagonism, and siVEGF delivery in vitro have been evaluated. The potential of PEI-C/siVEGF polyplexes as antitumor and antimetastatic treatment strategy that beneficially combines VEGF silencing with concordant CXCR4 inhibition was tested in a syngeneic mouse model of breast cancer.

2. MATERIALS AND METHODS

2.1. Materials. Cyclam (1,4,8,11-tetraazacyclotetradecane) was purchased from Vesina Industrial (Tianjin, China). Branched polyethylenimine (PEI, Mw 10 kDa) was obtained from Polysciences (Warrington, PA). Solvents (certified ACS) were purchased from Fisher (Fair Lawn, NJ) without further purification. AMD3100 (base form) was from Biochempartner (Shanghai, China). Fluorescently labeled FAM-siRNA (5′-UUCUCCGAACGUGUCACG UTT-3′), scrambled siRNA (siScr) and VEGF siRNA (5′-AUGUGAAUGC-AGACCAAAGAA-3′) were purchased from GenePharma (Shanghai, China). Dulbecco's phosphate buffered saline (PBS), trypsin, penicillin/streptomycin (Pen-Strep), RPMI-1640, Dulbecco's modified Eagle medium (DMEM), and fetal bovine serum (FBS) were from Hyclone (Waltham, MA). LysoTracker Red was from the Beyotime Institute of Biotechnology. Human SDF-1α was from Shenandoah Biotechnology, Inc. (Warwick, PA). VEGF mouse antibody, β-tubulin mouse antibody, and goat antimouse lgG-HRP were purchased from Santa Cruz Biotechnologies (Dallas, TX). All other reagents were from Nanjing Wanqing Chemical Glassware Instrument unless otherwise stated.

2.2. Synthesis and Characterization of PEI-C. The synthesis of tri-*tert*-butyl-11-(4-(chloromethyl)benzyl)-1,4,8,11-tetraazacyclotetradecane-1,4,8-tricarboxylate (cyclam derivative) was previously reported.[36] The conjugation of the cyclam derivative to PEI was achieved by nucleophilic substitution. The typical conjugation procedure is described as follows. Branched PEI (Mw 10 kDa, 258.6 mg), tri-*tert*-butyl-11-(4-(chloromethyl)benzyl)-1,4,8,11-tetraazacyclotetradecane-1,4,8-tricarboxylate (3.088 g, 4.8 mmol) and potassium carbonate (1.66 g, 12 mmol) were suspended in acetonitrile (20 mL) and refluxed for 16 h. The resulting product was filtered and evaporated. Trifluoroacetic acid (20 mL) was added and stirred overnight to perform deprotection. The final product was dialyzed against HCl (pH 3) for 2 days and water for an additional day before lyophilization. The typical yield was ∼75%. The composition of the polymer was characterized by ^{1}H NMR (Bruker 500 MHz) and analyzed by TopSpin 3.5pl6 software.

2.3. Preparation and Characterization of Polyplexes. Polyplexes were prepared by mixing equal volume of siRNA solution (20 μg/mL in 10 mM HEPES, pH 7.4) with polymers to achieve the desired w/w ratios. The mixture was vigorously vortexed for 30 s and incubated at room temperature for 30 min. To evaluate the ability of PEI-C to condense siRNA, polyplexes prepared at different PEI-C-to-siRNA weight ratios were run on 2% agarose gel containing JelRed at 100 V for 30 min and then visualized under UV illumination. Hydrodynamic diameter and zeta potential of the polyplexes were determined by Zeta Plus (Brookhaven Instruments Corp, Holtsville, NY).

2.4. Cell Culture. 4T1 cells (ATCC, Manassas, VA) were cultured in RPMI-1640 supplemented with 10% FBS and 1% Pen-Strep. Human epithelial osteosarcoma U2OS cells stably expressing functional EGFP-CXCR4 fusion protein (Fisher Scientific) were cultured in DMEM supplemented with 2 mM L-Glutamine, 10% FBS, 1% Pen-Strep, and 0.5 mg/mL G418. Mouse lung fibroblasts L929 cells were cultured in DMEM, supplemented with 10% fetal bovine serum and 1% Pen-Strep. All the cells were cultured at 37 °C in 5% CO_2 atmosphere.

2.5. Cytotoxicity. Cytotoxicity of the polymers was measured by MTT assay in 4T1, U2OS, and L929 cells. The cells were seeded in 96-well plates at a density of 8000 cells per well for 24 h and then incubated with serial dilutions of PEI and PEI-C for 24 h. Twenty microliters of MTT reagent was added and the cells were further incubated for 4 h. The medium was removed and 200 μL of DMSO was then added to each well. The absorbance [A] at 490 nm was measured using a microplate reader. The cell viability (%) was calculated as $([A]_{sample} - [A]_{blank})/([A]_{untreated} - [A]_{blank}) \times 100\%$.

2.6. Cellular Uptake and Intracellular Trafficking. Confocal microscopy was used to observe cellular uptake and intracellular trafficking of the polyplexes using FAM labeled siRNA. 4T1 cells were seeded into glass-bottom dishes at a density of 50,000 cells per dish. The cells were incubated for 18 h prior to use. The culture medium was then discarded and replaced by polyplexes in 1 mL of serum-free medium. The final concentration of siRNA was 100 nM. After 2 h incubation, the cells were washed three times with PBS, fixed with 4% paraformaldehyde for 20 min at room temperature, and the nuclei were stained by DAPI for 10 min. Cells were then visualized under a LSM700 confocal fluorescence microscope.

For determination of endosomal escape, cells were washed 3 times with PBS and stained with LysoTracker Red for 40 min after 2 or 6 h incubation with PEI-C/FAM-siRNA polyplexes. The cells were then washed 3 times with PBS and imaged by confocal microscopy.

2.7. CXCR4 Antagonism. U2OS cells stably expressing EGFP-CXCR4 fusion protein were seeded in 96-well black plates with optical bottom. Cells were washed twice with 100 μL of assay buffer (DMEM supplemented with 2 mM L-glutamine, 1% FBS, 1% Pen-Strep, and 10 mM HEPES) and treated with polymers (2 μg/mL) or AMD3100 (300 nM) for 30 min. Ten nanomolar SDF-1 was then added to each well and incubated for an additional 1 h. Cells were fixed with 4% paraformaldehyde for 20 min, washed with PBS for 4 times, and the nuclei were stained with 1 μM Hoechst 33258 for 30 min. Cells were imaged using EVOS fl microscope.

2.8. Cell Invasion. The transwell inserts in 24-well plates were coated with 40 μL of diluted Matrigel (1:3 v/v with serum-free medium) and then placed in 37 °C incubator for 2 h. Thirty thousand 4T1 cells were trypsinized, washed, and resuspended in serum-free media containing PEI-C (2 μg/mL), PEI-C/siRNA polyplex (w/w 3) or AMD3100 (300 nM) for 30 min before adding to the insets. SDF-1 (20 nM) was applied as the chemoattractant and added to the companion 24-well plates. After 24 h of incubation, the noninvaded cells on the top side of the insets were removed using a cotton swab, and the migrated cells at the bottom side were fixed with 100% methanol and stained with 0.2% crystal violet for 10 min. Cells were imaged and counted using EVOS xl microscope. Results were expressed as percent of invaded cells ± SD (n = 3) using untreated cells as a control.

2.9. VEGF Silencing by Western Blot. 4T1 cells were seeded into 12-well plates (1×10^5 cells per well) 1 day prior to the transfection. The cells were incubated with PEI-C37/siVEGF or PEI-C37/siScr (final siRNA concentration 100 nM) in serum-free medium for 4 h. The polyplexes were then removed and the cells were further cultured in fresh culture medium for 48 h. To measure VEGF protein level after siRNA transfection, cells were first washed twice with cold PBS, and then lysed with RIPA lysis buffer containing protease and phosphatase inhibitors. After centrifugation at 12 000× g for 15 min, the protein concentration was quantified by BCA assay kit (Beyotime,

DOI: 10.1021/acs.biomac.7b01487
Biomacromolecules XXXX, XXX, XXX−XXX

China). Collected protein in the cell lysate was then separated by 10% SDS-polyacrylamide gel electrophoresis (SDS-PAGE) at 120 V for 2 h, and transferred to a nitrocellulose membrane. After 1 h of blocking procedure in 5% nonfat milk at room temperature, the membrane was probed with mouse primary anti-VEGF antibody overnight at 4 °C. Following incubation with the secondary antimouse IgG-HRP antibody for 2 h, the membrane was washed and visualized after incubating with Pierce ECL Western Blotting Substrate (Thermo Scientific, U.S.A.).

2.10. Anticancer Activity in Vivo. Female BALB/c mice (7 weeks old, 20−25 g) were supplied by the Experimental Animal Centre of Yangzhou University (Yangzhou, China). All animals were treated following protocols approved by the ethical committee of China Pharmaceutical University. 4T1 cells (10^5) suspended in 100 μL of PBS were injected into the mammary fat pad of the mice and allowed to grow for 10 days. The mice were then randomized into three experimental groups (n = 5): saline, PEI-C/siScr, and PEI-C/siVEGF polyplexes. The polyplexes were prepared at w/w 6 and administered by direct intratumoral injection (20 μg siRNA/mouse). The day of the first administration was designated as day 0. Polyplexes were given for a total 4 doses at a 3-day interval (Day 0, 3, 6, and 9). Body weight and tumor size of mice were monitored and recorded every other day. All the animals were sacrificed at Day 16, and tumors and lungs were collected and processed for H&E staining and immunohistochemistry (IHC) analysis.

3. RESULTS AND DISCUSSION

We have previously reported the development of poly(amido amine) polycations for simultaneous delivery of nucleic acids and CXCR4 inhibition to treat metastatic cancer. We have shown that using small-molecule cyclam CXCR4 antagonists as the polymer building blocks equips the polymers with strong antimetastatic activity, while preserving the ability to form polyplexes with nucleic acids. We have reported synthesis of both degradable and nondegradable poly(amido amine)s.[35,36,39] In the original design, the cationic cyclam moieties provided both the CXCR4 inhibition and nucleic acid binding, thus shouldering the burden of providing both biological functions and potentially compromising the overall activity. In this study, we designed and developed a new class of CXCR4-inhibiting polycations by conjugating our recently developed cyclam CXCR4 antagonist to PEI, a well-studied polycation for delivering therapeutic nucleic acids. We hypothesized that the proposed polymer design will allow us to better combine CXCR4 antagonism and siRNA delivery in a single molecule, thus representing a simple way to introduce an additional antimetastatic function to existing carrier (Scheme 1).

3.1. Synthesis of PEI-C. A series of cyclam modified PEI (PEI-C) were synthesized by nucleophilic substitution of PEI with the developed cyclam derivative (1) (Scheme 2). To synthesize the Boc-protected cyclam derivative (tri-*tert*-butyl-11-(4-(chloromethyl)benzyl)-1,4,8,11-tetraazacyclotetradecane-1,4,8-tricarboxylate) we have followed our previously published procedure.[36] To prepare PEI-C, we selected branched PEI with molecular weight 10 kDa due to its favorable safety profile.[40−43] In a typical conjugation procedure, PEI was refluxed with (1) in acetonitrile in the presence of K_2CO_3. The resulting product was collected by filtration and the Boc protecting groups from cyclam were removed by trifluoroacetic acid. The final PEI-C product was then obtained as a hydrochloride salt by lyophilization after dialyzing against HCl-acidified water. We obtained typical yield around 75%. The content of cyclam in PEI-C was calculated using ^{1}H NMR, by comparing the signal of the protons on the phenylene ring (δ 6.7−7.6) in (1) to the signal of the PEI ethylene groups (δ 2.1−2.9) (Figure 1). Three

Scheme 1. Mechanism of Action of PEI-C/siVEGF Polyplexes

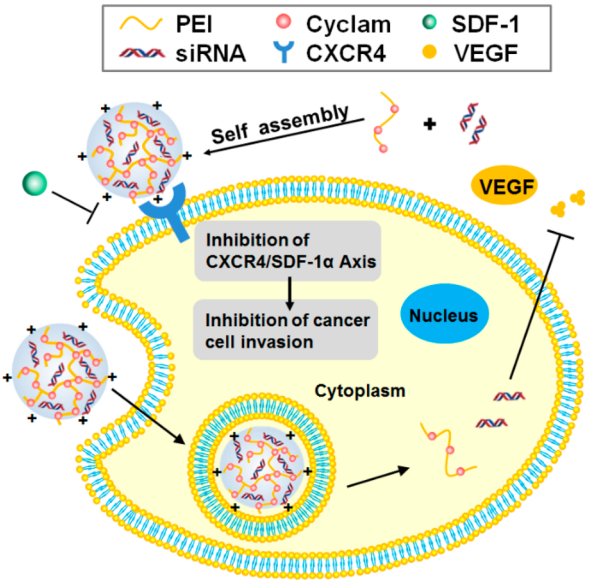

PEI-C polymers with increasing cyclam content were synthesized and named based on the conjugation ratio. The conjugation ratio and cyclam content (mol %) in feed and in the product of all the PEI-C were summarized in Table 1. In general, the cyclam content in the polymer increased with increasing feed content of (1). However, when the feed ratio doubled in the case of PEI-C37 when comparing with PEI-C33 (80 vs 40 mol %), the cyclam content in the synthesized polymer only increased slightly (25 vs 27 mol %). This is most likely due to the hyperbranched architecture of the PEI and the related steric hindrance, which reduced accessibility of the amines for alkylation with (1).

3.2. Cytotoxicity. Despite its superior gene delivery efficiency, PEI is also notorious for its cytotoxicity and hemolytic activity.[40−42,44] Before we proceeded to evaluate the biological activity of PEI-C, MTT assay was used to examine the cytotoxicity of PEI-C in mouse breast cancer 4T1 cells, EGFP-CXCR4 + U2OS (model cell line to study CXCR4 antagonism) and normal mouse lung fibroblasts L929 cells. PEI was included as a control. The cell viability curves and calculated IC50 values of all the polymers are summarized in Figure 2. All the PEI-C polymers showed reduced cytotoxicity when compared with PEI in all cell lines as indicated by the increased IC50 values. In addition, the PEI-C cytotoxicity decreased with increasing cyclam content in the polymer. PEI-C37, which contains the highest cyclam content, showed the highest IC50 values among all the tested polymers. The observed IC50 of PEI-C37 was ~23-fold higher than PEI in 4T1 cells and ~10-fold higher than PEI in U2OS cells. In L929 cells, used as an example of noncancerous normal cells, the cell viability remained above 80% even after treatment with 100 μg/mL PEI-C. The IC50 of PEI-C was above 600 μg/mL. This result suggested that PEI-C polymers may show selective cytotoxicity in tumor cells due to their CXCR4-mediated effects.

Every third atom in the PEI chemical structure is a protonizable amine, giving the polymer high charge density and outstanding buffering capacity over a wide pH range. Such high cationic charge density, however, becomes a double-edged

DOI: 10.1021/acs.biomac.7b01487
Biomacromolecules XXXX, XXX, XXX−XXX

Scheme 2. Synthesis of PEI-C[a]

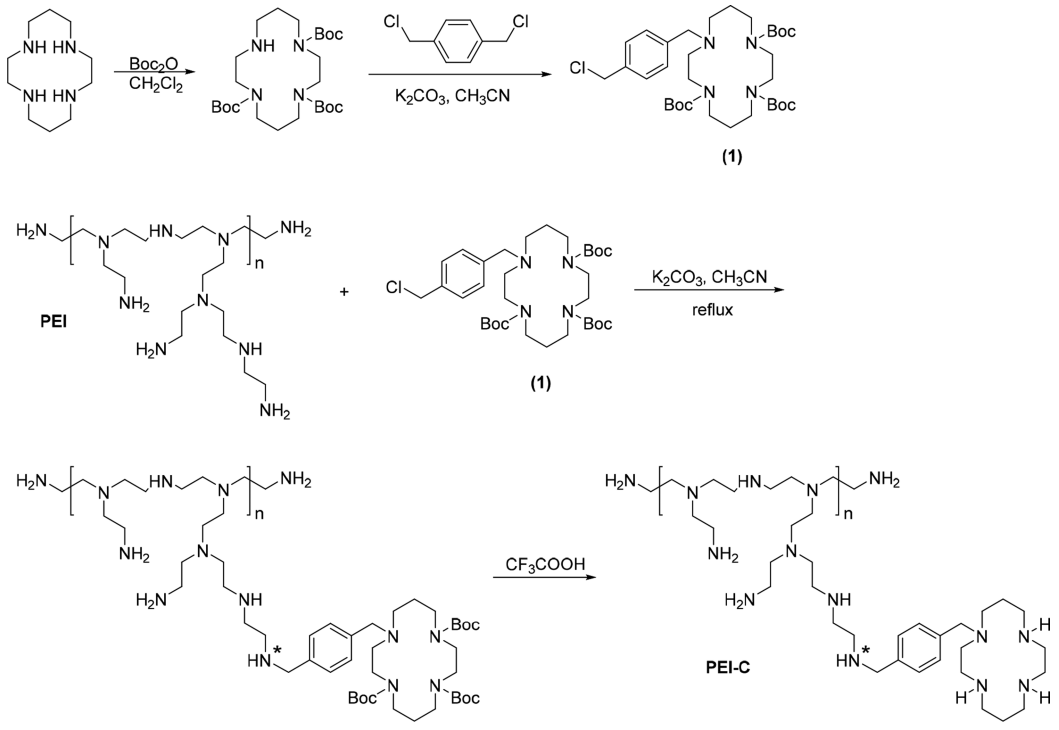

[a]Could be any primary, secondary, or tertiary amine.

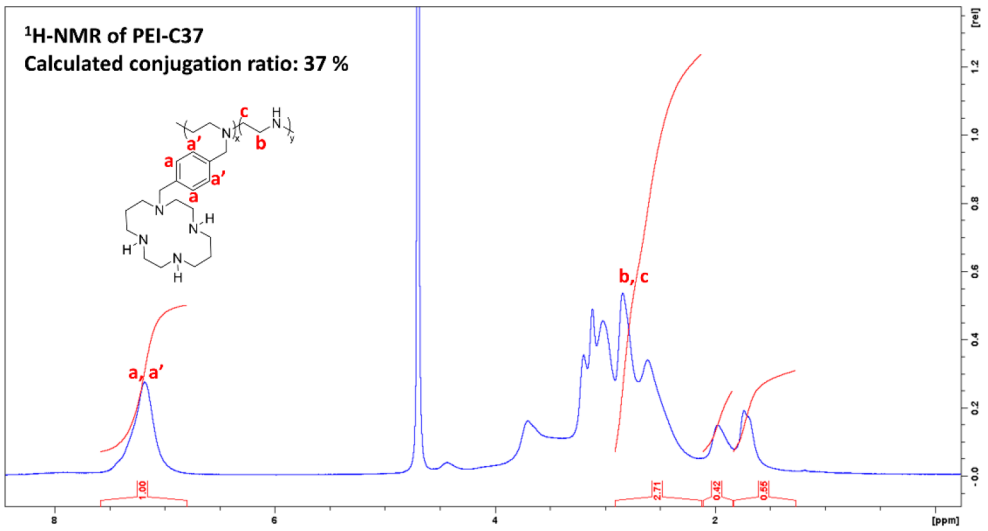

Figure 1. Typical ^{1}H NMR spectrum of PEI-C (PEI-C37 in D_2O) used in the determination of the cyclam content. Integration of the proton on the aromatic ring (a and a′) and on the unconjugated ethylenimine (b,c) were used for the calculations of the conjugation ratio.

Table 1. Characterization Summary of PEI-C

polymer	conjugation ratio (mol %)[a]	cyclam content (mol %) in feed	cyclam content (mol %) in polymer	Mw (kDa)
PEI	0	0	0	10.0
PEI-C22	22	30	18	20.8
PEI-C33	33	40	25	24.1
PEI-C37	37	80	27	25.0

[a]Conjugation ratio (mol %) is defined as the ratio of conjugated ethylenimines to unconjugated ethylenimines based on 1H-NMR.

sword. The high protonation degree of PEI at physiological pH provides high binding and complexation with negatively charged nucleic acids due to electrostatic interactions but also leads to nonspecific interactions and perturbations of lipid bilayers in cell membranes, thus causing toxicity.[45−47] Cyclam, on the other hand, has a complex and unusual protonation behavior as suggested by the pK_a of the four amines: 11.29, 10.19, 1.61 and 1.91.[48] Only two out of the four amines can be protonated at physiological pH. After cyclam modification, the fraction of protonated amines in PEI-C thus decreases significantly, resulting in decreased overall cationic charge density of the polymer. Such reduction in charge density also becomes more pronounced when the cyclam content is

DOI: 10.1021/acs.biomac.7b01487
Biomacromolecules XXXX, XXX, XXX−XXX

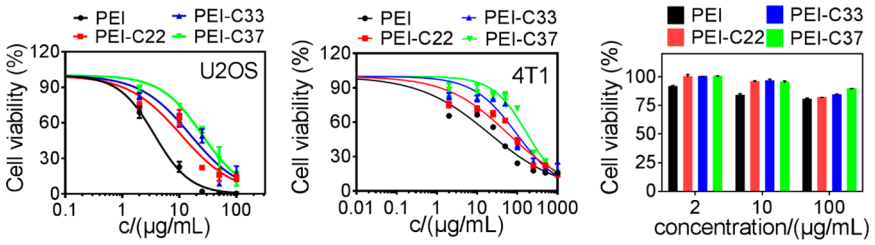

IC50 (μg/mL)	PEI	PEI-C22	PEI-C33	PEI-C37
U2OS	3.7	12.8	23.1	39.9
4T1	11.9	64.8	142.6	278.3

Figure 2. Cytotoxicity of PEI-C in U2OS, 4T1, and L929 cells. Cells were incubated with increasing concentrations of polymers for 24 h before measuring cell viability by MTT assay. IC50 values were calculated.

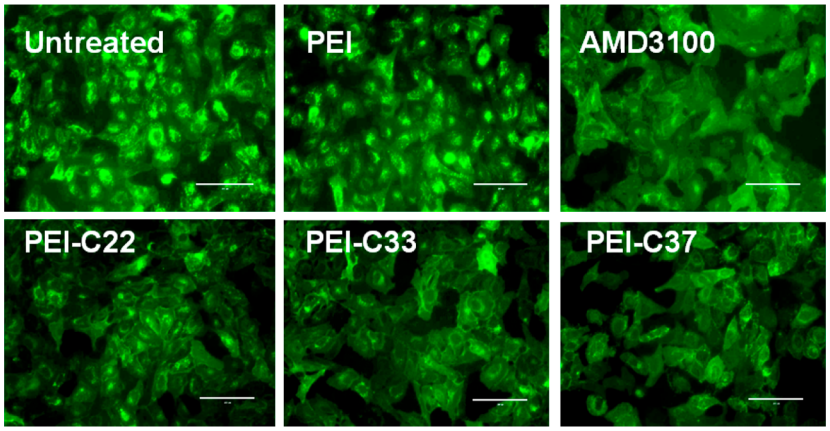

Figure 3. CXCR4 antagonism of PEI-C. U2OS overexpressing EGFP-CXCR4 cells were treated with PEI-C for 30 min before incubation with 10 nM SDF-1. AMD3100 (300 nM) was used as a positive control.

increased. The specific binding of cyclam moiety and cell surface CXCR4 receptors might also alter the cellular uptake pathways and contribute to the reduced toxicity.

3.3. CXCR4 Antagonism. After the safe dosing range of PEI-C was determined, we investigated the CXCR4 antagonistic ability of the polymers using a phenotypic CXCR4 receptor redistribution assay.[35] This assay can be applied to track and visualize the translocation of EGFP-tagged CXCR4 receptors on the cell membrane to endosomes upon ligand (SDF-1) stimulation, which is a typical behavior for G-protein coupled receptors. As shown in Figure 3, untreated cells exhibited CXCR4 translocation as indicated by the enhanced green fluorescent signals inside the cells with minimal visible signal on the plasma membrane. Cells that were treated with CXCR4 antagonist AMD3100 exhibited a diffused pattern of green fluorescence, indicating the inhibition of CXCR4 translocation after SDF-1 stimulation. All the PEI-C (2 μg/mL) demonstrated strong CXCR4 inhibition when compared with unmodified PEI. PEI-C37 with the highest cyclam content appears to show the best CXCR4 inhibition. Our results confirmed that PEI-C function as CXCR4 antagonists after nondegradable conjugation of the cyclam moiety onto the PEI polymer.[36,39]

3.4. Cell Invasion. Binding of SDF-1 and CXCR4 initiates downstream signaling that leads to intracellular calcium flux, chemotaxis, cell survival, and proliferation.[49−51] Blocking the CXCR4/SDF-1 axis using CXCR4 antagonists has been reported to significantly abrogate cell migration and reduce tumor metastasis in breast cancer.[16,49,51] After we confirmed the CXCR4 antagonistic activity of PEI-C, the efficiency to inhibit CXCR4/SDF-1 axis modulated cancer cell migration was further evaluated using 4T1 mouse breast cancer cells. A Boyden chamber cell migration setting was applied and SDF-1 (20 nM) was used as the chemoattractant. As shown in Figure 4, AMD3100 exhibited marked inhibition of cell migration (75%). All the PEI-C (2 μg/mL) achieved enhanced inhibitory activity (88−92% cell migration inhibition) when compared with AMD3100. PEI-C polyplexes (w/w 3) showed slightly improved cell migration inhibition (91−93%) compared with PEI-C polymer due to significant amount of free polycation. PEI (2 μg/mL) showed minimal inhibition of cell migration (~25%), which might be related to nonspecific interactions between PEI and cell membrane receptors involved in cell migration.

3.5. Preparation and Characterization of the Polyplexes. The ability of PEI-C to complex siRNA was determined by agarose gel electrophoresis. The polyplexes were prepared at increasing PEI-C to siRNA w/w ratios. As shown in Figure 5A, unmodified PEI could fully complex the siRNA at w/w ratios as low as 1. All the PEI-C polymers exhibited complete siRNA complexation at w/w 1.5, while leaving traces of free siRNA at w/w 1. This again could be

DOI: 10.1021/acs.biomac.7b01487
Biomacromolecules XXXX, XXX, XXX−XXX

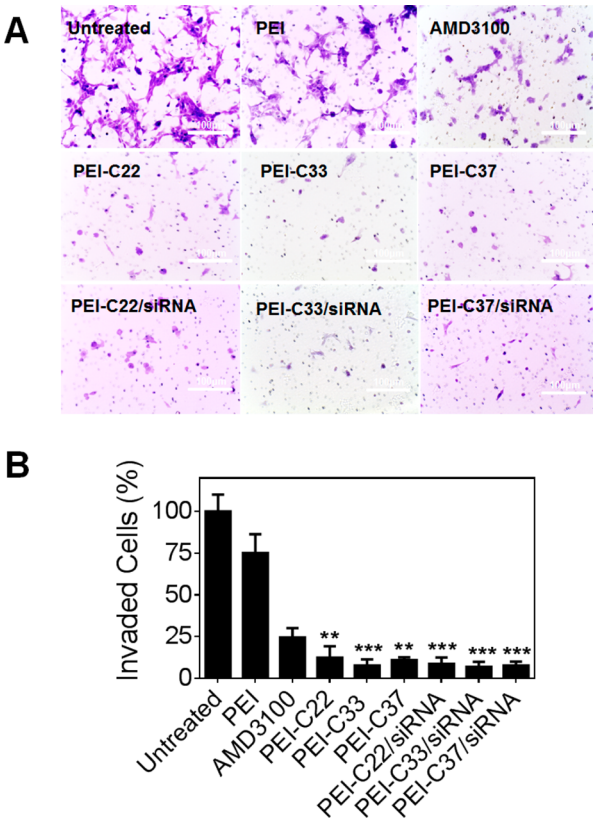

Figure 4. Inhibition of cancer cell invasion. (A) 4T1 cells were treated with PEI-C (200 nM), PEI-C polyplexes (w/w 3), and allowed to invade through Matrigel for 24 h. AMD3100 (300 nM) was used as a positive control and PEI was used as a negative control. (B) The percent of invaded 4T1 cells. Results shown as mean percent of invaded cells using untreated cells as 100% ± SD (n = 3). (**p < 0.01, ***p < 0.001 vs AMD3100).

attributed to the unique protonation constants of the cyclams. Hydrodynamic sizes and zeta potential of PEI-C/siRNA polyplexes were evaluated by dynamic light scattering at w/w 3, 6, and 9 (Figure 5B,C). The sizes of all the PEI-C/siRNA polyplexes were around 100 nm in diameter (ranging from 62 to 114 nm) with positive surface charge (ranging from 25 to 53 mV). No substantial differences in either size or surface charge were observed between PEI-C and PEI.

3.6. Cellular Uptake. Small molecule CXCR4 antagonists like AMD3100 exert their biological activity by competitively binding with the CXCR4 at the plasma membrane to prevent them from internalization and triggering intracellular signaling cascade. However, for polymeric CXCR4 antagonists to achieve dual functions as both CXCR4 inhibitors and efficient delivery vectors of nucleic acids, the polyplexes are required to be internalized inside the cells. Here we used fluorescently labeled siRNA (FAM-siRNA, green) to monitor the cell uptake of the PEI-C/siRNA polyplexes. The 4T1 cells were treated with PEI-C/FAM-siRNA prepared at w/w 3 for 2 h before visualization by confocal microscopy. Cell nuclei were stained with DAPI (blue). As shown in Figure 6A, a significant amount of green fluorescent signal was observed in the cytoplasm for all the polyplexes compared with naked FAM-siRNA. No notable differences were observed between the PEI-C and PEI polyplexes, which confirmed the delivery function of PEI was preserved after cyclam modification with no compromise in the cellular uptake of siRNA.

We then determined the endosomal escape of PEI-C/FAM-siRNA using confocal microscopy. The 4T1 cells were incubated with the polyplexes for 2 and 6 h and lysosomes were stained with LysoTrackerRed. After incubation for 2 h, the green fluorescence of FAM-siRNA overlaid with the red LysoTracker signal, suggesting that most of the endocytosed FAM-siRNA was localized in the lysosomes. After 6 h, notable separation between green fluorescence of FAM-siRNA and the red signal of LysoTracker Red was clearly noted, indicating that FAM-siRNA had successfully escaped from the endosomes.

3.7. Transfection and VEGF Silencing in Vitro. Cyclam modification of PEI has shown no negative effect on cellular uptake of siRNA. Only marginal differences were observed in

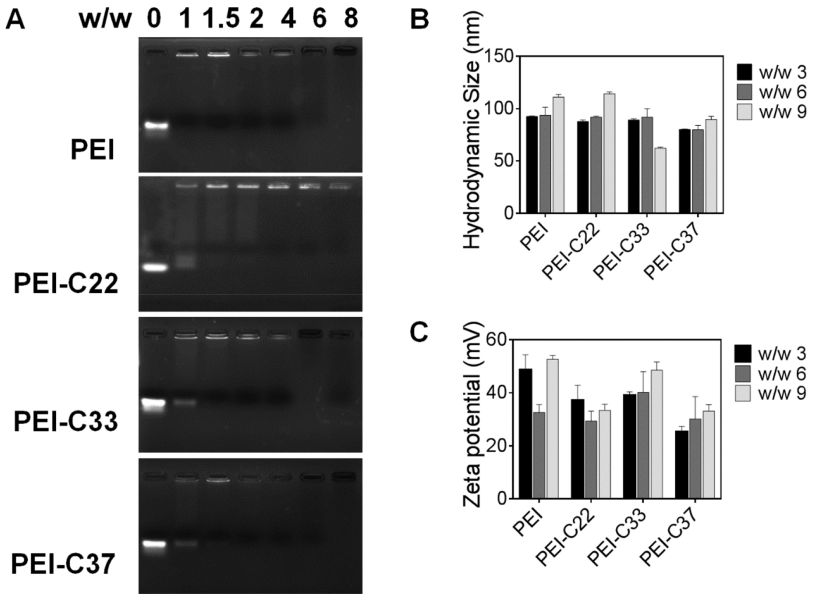

Figure 5. Physicochemical characterization of PEI-C/siRNA polyplexes. (A) siRNA complexation by agarose gel electrophoresis. (B) Hydrodynamic size and (C) zeta potential of polyplexes at various w/w ratios. Data shown as mean ± SD (n = 3).

DOI: 10.1021/acs.biomac.7b01487
Biomacromolecules XXXX, XXX, XXX−XXX

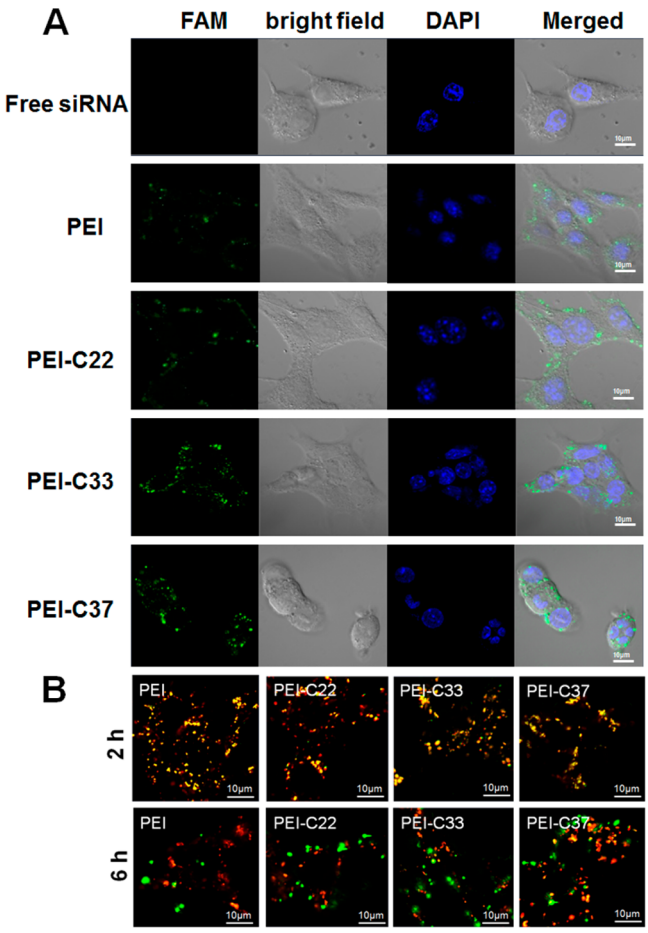

Figure 6. (A) Cellular uptake of polyplexes in 4T1 cells by confocal microscopy after 2 h of incubation using FAM-siRNA (green). The nuclei are stained with DAPI (blue). (B) Endosomal escape of PEI-C polyplexes (w/w 3) in 4T1 cells for 2 and 6 h incubation. Lysosomes were stained with Lysotracker Red.

the CXCR4 antagonism and cell migration inhibition among all the PEI-C polymers. Therefore, we selected PEI-C37, which exhibited the lowest cytotoxicity to further investigate siRNA transfection and VEGF silencing effect in vitro. The 4T1 cells were transfected with PEI-C37/siVEGF and PEI-C37/siScr polyplexes at w/w 3 (final siRNA concentration 100 nM), and VEGF expression was analyzed by Western blot 48 h post-transfection. As shown in Figure 7, PEI-C37/siVEGF

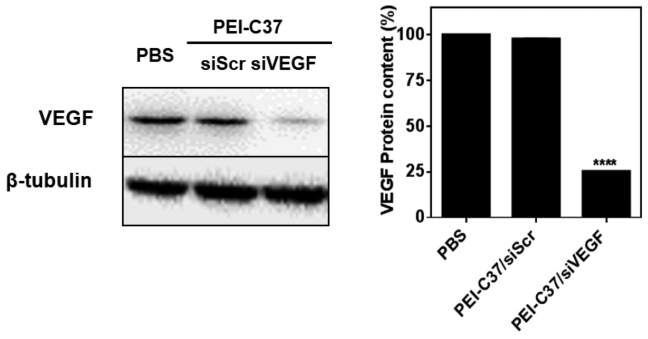

Figure 7. VEGF protein silencing by PEI-C37/siVEGF polyplexes in 4T1 cells by Western blot. Quantification of the bands was performed using ImageJ software.

demonstrated robust VEGF silencing in 4T1 cells, giving 75% knockdown of VEGF protein expression when compared with negative control PEI-C37/siScr. These results confirmed efficient siVEGF delivery in vitro and provided support for testing in vivo anticancer activity.

3.8. Anticancer Activity in Vivo. The anticancer and antimetastatic activity of PEI-C37/siVEGF polyplexes was evaluated using orthotopic metastatic breast cancer mouse model. A total of 10^5 4T1 cells were injected subcutaneously into the mammary fat pad of female Balb/C mice and allowed to form palpable tumors. Tumor size was monitored closely until reaching 100 mm^3. All the tumor-bearing mice were then randomized into three different groups (n = 5) and intratumorally administered with (i) saline, (ii) PEI-C37/siScr, and (iii) PEI-C37/siVEGF. As shown in Figure 8A, no significant body weight loss was observed throughout the treatment, indicating minimal toxicity of the polyplexes. PEI-C37/siVEGF exhibited marked decrease in tumor growth compared with the saline group (Figure 8B). Treatment with PEI-C37/siScr also slowed down the primary tumor growth, which could be attributed to the CXCR4 antagonism of PEI-C37 as inhibition of CXCR4 regulates cell growth and proliferation. At the concluding day of the experiment, primary tumors (Figure 8C) and lungs (Figure 8D) were harvested. As shown in Figure 8D, compared with the saline-treated group, which showed extensive metastasis in the lung, no significant metastasis was observed in the animals treated with either the PEI-C37/siScr or PEI-C37/siVEGF. H&E staining of the lung sections was further performed (Figure 8F) and the number of lung metastatic lesions was counted (Figure 8E) to validate the antimetastatic activity of PEI-C37. To investigate the in vivo siRNA delivery efficiency by PEI-C37, tumor tissue slides were stained with CD31, an endothelial cell-specific surface marker to detect disorganized vascular endothelium and angiogenesis in the tumor. Tumors treated with the PEI-C37/siVEGF polyplexes showed marked reduction in tumor vasculature compared with saline and PEI-C37/siScr groups, indicating significant inhibition of tumor angiogenesis. These results provide important in vivo evidence that PEI modified with cyclam-based CXCR4 antagonists is capable of simultaneously delivering therapeutic siVEGF and inhibiting CXCR4-regulated tumor growth and metastasis, thus achieving beneficial combinational anticancer activity.

■ CONCLUSIONS

In this study, we developed a new polycationic CXCR4 antagonists based on PEI (PEI-C) that can simultaneously deliver VEGF siRNA and inhibit CXCR4/SDF-1 axis to achieve combination anticancer therapy in metastatic breast cancer. Our results confirmed that conjugation of cyclam-based CXCR4 antagonists to PEI is able to (i) retain the siRNA delivery efficiency of PEI, (ii) decrease the cytotoxicity of PEI, and (iii) exert CXCR4 antagonism and inhibition of CXCR4-mediated cancer cell invasion. The PEI-C/siVEGF polyplexes demonstrated combination antimetastatic and anticancer activity due to the simultaneous CXCR4 inhibition and VEGF silencing. The reported PEI modification represents a simple approach to introducing a new pharmacologic function to existing siRNA delivery vectors in order to achieve enhanced delivery and therapeutic efficiency for potential antitumor and antimetastatic applications.

DOI: 10.1021/acs.biomac.7b01487
Biomacromolecules XXXX, XXX, XXX−XXX

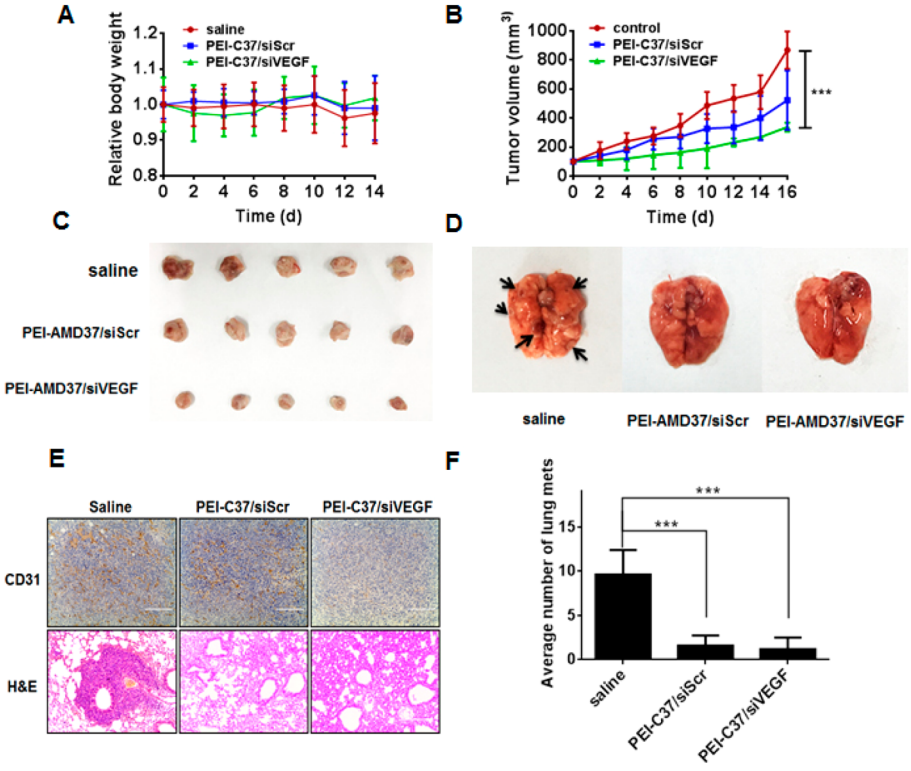

Figure 8. Anticancer activity of PEI-C37/siRNA polyplexes in 4T1 metastatic breast cancer mouse model. (A) Body weight change of the mice after different treatments. (B) Tumor growth curves of different treatment groups. Results are shown as average of tumor volume ± SD (n = 5, ***p < 0.001). (C) Photograph of primary tumors harvested after sacrificing the animals at the end of the experiment. (D) Photograph of representative lungs from each treatment group. Visible surface metastases were indicated by black arrows. (E) CD31 immunohistochemistry staining of primary tumors and H&E staining of lungs. (F) Average number of metastases on lung tissue sections. Results are shown as average number of lung metastases ± SD (n = 5, ***p < 0.001).

AUTHOR INFORMATION

Corresponding Author

*E-mail: david.oupicky@unmc.edu.

ORCID

Minjie Sun: 0000-0003-0582-6189

David Oupický: 0000-0003-4710-861X

Author Contributions

§Y.Z. and F.Y. contributed equally to the manuscript.

Notes

The authors declare no competing financial interest.

ACKNOWLEDGMENTS

This work was financially supported by the National Science and Technology Major Project (2017YFA0205400), Changjiang Scholar program from the Chinese Ministry of Education, University of Nebraska Medical Center, China National Science Foundation (81373983, 81573377), China Postdoctoral Science Foundation (No. 2016M601923), and the National Institutes of Health (EB020308).

REFERENCES

(1) Skobe, M.; Hawighorst, T.; Jackson, D. G.; Prevo, R.; Janes, L.; Velasco, P.; Riccardi, L.; Alitalo, K.; Claffey, K.; Detmar, M. Induction of tumor lymphangiogenesis by VEGF-C promotes breast cancer metastasis. *Nat. Med.* **2001**, *7* (2), 192−198.

(2) Park, K.; Lee, M.-Y.; Kim, K. S.; Hahn, S. K. Target specific tumor treatment by VEGF siRNA complexed with reducible polyethyleneimine-hyaluronic acid conjugate. *Biomaterials* **2010**, *31* (19), 5258−5265.

(3) Kim, S. H.; Jeong, J. H.; Lee, S. H.; Kim, S. W.; Park, T. G. Local and systemic delivery of VEGF siRNA using polyelectrolyte complex micelles for effective treatment of cancer. *J. Controlled Release* **2008**, *129* (2), 107−116.

(4) Duda, D. G.; Kozin, S. V.; Kirkpatrick, N. D.; Xu, L.; Fukumura, D.; Jain, R. K. CXCL12 (SDF1α)-CXCR4/CXCR7 Pathway Inhibition: An Emerging Sensitizer for Anticancer Therapies? *Clin. Cancer Res.* **2011**, *17* (8), 2074−2080.

(5) Jung, K.; Heishi, T.; Incio, J.; Huang, Y.; Beech, E. Y.; Pinter, M.; Ho, W. W.; Kawaguchi, K.; Rahbari, N. N.; Chung, E.; Kim, J. K.; Clark, J. W.; Willett, C. G.; Yun, S. H.; Luster, A. D.; Padera, T. P.; Jain, R. K.; Fukumura, D. Targeting CXCR4-dependent immunosuppressive Ly6Clow monocytes improves antiangiogenic therapy in colorectal cancer. *Proc. Natl. Acad. Sci. U. S. A.* **2017**, *114* (39), 10455−10460.

(6) Barone, A.; Sengupta, R.; Warrington, N. M.; Smith, E.; Wen, P. Y.; Brekken, R. A.; Romagnoli, B.; Douglas, G.; Chevalier, E.; Bauer, M. P.; et al. Combined VEGF and CXCR4 antagonism targets the GBM stem cell population and synergistically improves survival in an intracranial mouse model of glioblastoma. *Oncotarget* **2014**, *5* (20), 9811−9822.

(7) Liu, C.-H.; Chan, K.-M.; Chiang, T.; Liu, J.-Y.; Chern, G.-G.; Hsu, F.-F.; Wu, Y.-H.; Liu, Y.-C.; Chen, Y. Dual-Functional Nanoparticles Targeting CXCR4 and Delivering Antiangiogenic siRNA Ameliorate Liver Fibrosis. *Mol. Pharmaceutics* **2016**, *13* (7), 2253−2262.

(8) Liu, J.-Y.; Chiang, T.; Liu, C.-H.; Chern, G.-G.; Lin, T.-T.; Gao, D.-Y.; Chen, Y. Delivery of siRNA using CXCR4-targeted nanoparticles modulates tumor microenvironment and achieves a potent antitumor response in liver cancer. *Mol. Ther.* **2015**, *23* (11), 1772−1782.

DOI: 10.1021/acs.biomac.7b01487
Biomacromolecules XXXX, XXX, XXX−XXX

(9) Bi, M. M.; Shang, B.; Wang, Z.; Chen, G. Expression of CXCR4 and VEGF-C is correlated with lymph node metastasis in non-small cell lung cancer. *Thorac. Cancer* **2017**, *8* (6), 634−641.
(10) Hao, L.; Zhang, C.; Qiu, Y.; Wang, L.; Luo, Y.; Jin, M.; Zhang, Y.; Guo, T. B.; Matsushima, K.; Zhang, Y. Recombination of CXCR4, VEGF, and MMP-9 predicting lymph node metastasis in human breast cancer. *Cancer Lett.* **2007**, *253* (1), 34−42.
(11) Liang, Z.; Wu, T.; Lou, H.; Yu, X.; Taichman, R. S.; Lau, S. K.; Nie, S.; Umbreit, J.; Shim, H. Inhibition of breast cancer metastasis by selective synthetic polypeptide against CXCR4. *Cancer Res.* **2004**, *64* (12), 4302−4308.
(12) Guo, P.; You, J.-O.; Yang, J.; Jia, D.; Moses, M. A.; Auguste, D. T. Inhibiting Metastatic Breast Cancer Cell Migration via the Synergy of Targeted, pH-triggered siRNA Delivery and Chemokine Axis Blockade. *Mol. Pharmaceutics* **2014**, *11* (3), 755−765.
(13) Smith, M. C.; Luker, K. E.; Garbow, J. R.; Prior, J. L.; Jackson, E.; Piwnica-Worms, D.; Luker, G. D. CXCR4 regulates growth of both primary and metastatic breast cancer. *Cancer Res.* **2004**, *64* (23), 8604−8612.
(14) Wang, Y.; Li, J.; Oupicky, D. Polymeric Plerixafor: Effect of PEGylation on CXCR4 Antagonism, Cancer Cell Invasion, and DNA Transfection. *Pharm. Res.* **2014**, *31* (12), 3538−3548.
(15) Wang, Y.; Xie, Y.; Oupicky, D. Potential of CXCR4/CXCL12 Chemokine Axis in Cancer Drug Delivery. *Curr. Pharmacol Rep.* **2016**, *2* (1), 1−10.
(16) Huang, E. H.; Singh, B.; Cristofanilli, M.; Gelovani, J.; Wei, C.; Vincent, L.; Cook, K. R.; Lucci, A. A CXCR4 antagonist CTCE-9908 inhibits primary tumor growth and metastasis of breast cancer. *J. Surg. Res.* **2009**, *155* (2), 231−236.
(17) Gerlach, L. O.; Skerlj, R. T.; Bridger, G. J.; Schwartz, T. W. Molecular interactions of cyclam and bicyclam non-peptide antagonists with the CXCR4 chemokine receptor. *J. Biol. Chem.* **2001**, *276* (17), 14153−14160.
(18) McManus, M. T.; Sharp, P. A. Gene silencing in mammals by small interfering RNAs. *Nat. Rev. Genet.* **2002**, *3* (10), 737−747.
(19) Shiver, J. W.; Fu, T.-M.; Chen, L.; Casimiro, D. R.; Davies, M.-E.; Evans, R. K.; Zhang, Z.-Q.; Simon, A. J.; Trigona, W. L.; Dubey, S. A.; et al. Replication-incompetent adenoviral vaccine vector elicits effective anti-immunodeficiency-virus immunity. *Nature* **2002**, *415* (6869), 331−335.
(20) Dykxhoorn, D. M.; Novina, C. D.; Sharp, P. A. Killing the messenger: short RNAs that silence gene expression. *Nat. Rev. Mol. Cell Biol.* **2003**, *4* (6), 457−467.
(21) Song, E.; Lee, S.-K.; Wang, J.; Ince, N.; Ouyang, N.; Min, J.; Chen, J.; Shankar, P.; Lieberman, J. RNA interference targeting Fas protects mice from fulminant hepatitis. *Nat. Med.* **2003**, *9* (3), 347−351.
(22) Xiong, X.-B.; Uludağ, H.; Lavasanifar, A. Biodegradable amphiphilic poly (ethylene oxide)-block-polyesters with grafted polyamines as supramolecular nanocarriers for efficient siRNA delivery. *Biomaterials* **2009**, *30* (2), 242−253.
(23) Lachelt, U.; Wagner, E. Nucleic Acid Therapeutics Using Polyplexes: A Journey of 50 Years (and Beyond). *Chem. Rev.* **2015**, *115* (19), 11043−11078.
(24) Chen, G.; Wang, K.; Wu, P.; Wang, Y.; Zhou, Z.; Yin, L.; Sun, M.; Oupický, D. Development of fluorinated polyplex nanoemulsions for improved small interfering RNA delivery and cancer therapy. *Nano Res.* **2017**, DOI: 10.1007/s12274-017-1946-z.
(25) Merkel, O. M.; Kissel, T. Quo vadis polyplex? *J. Controlled Release* **2014**, *190* (0), 415−423.
(26) He, H.; Bai, Y.; Wang, J.; Deng, Q.; Zhu, L.; Meng, F.; Zhong, Z.; Yin, L. Reversibly cross-linked polyplexes enable cancer-targeted gene delivery via self-promoted DNA release and self-diminished toxicity. *Biomacromolecules* **2015**, *16* (4), 1390−1400.
(27) Shim, M. S.; Kwon, Y. J. Acid-responsive linear polyethylenimine for efficient, specific, and biocompatible siRNA delivery. *Bioconjugate Chem.* **2009**, *20* (3), 488−499.
(28) Bonnet, M.-E.; Erbacher, P.; Bolcato-Bellemin, A.-L. Systemic delivery of DNA or siRNA mediated by linear polyethylenimine (L-PEI) does not induce an inflammatory response. *Pharm. Res.* **2008**, *25* (12), 2972−2982.
(29) Dehshahri, A.; Oskuee, R. K.; Shier, W. T.; Hatefi, A.; Ramezani, M. Gene transfer efficiency of high primary amine content, hydrophobic, alkyl-oligoamine derivatives of polyethylenimine. *Biomaterials* **2009**, *30* (25), 4187−4194.
(30) Breunig, M.; Lungwitz, U.; Liebl, R.; Goepferich, A. Breaking up the correlation between efficacy and toxicity for nonviral gene delivery. *Proc. Natl. Acad. Sci. U. S. A.* **2007**, *104* (36), 14454−14459.
(31) Chen, G.; Wang, K.; Wang, Y.; Wu, P.; Sun, M.; Oupický, D. Fluorination Enhances Serum Stability of Bioreducible Poly (amido amine) Polyplexes and Enables Efficient Intravenous siRNA Delivery. *Adv. Healthcare Mater.* **2017**, 1700978 DOI: 10.1002/adhm.201700978.
(32) Chen, G.; Wang, K.; Hu, Q.; Ding, L.; Yu, F.; Zhou, Z.; Zhou, Y.; Li, J.; Sun, M.; Oupický, D. Combining Fluorination and Bioreducibility for Improved siRNA Polyplex Delivery. *ACS Appl. Mater. Interfaces* **2017**, *9* (5), 4457−4466.
(33) Masotti, A.; Moretti, F.; Mancini, F.; Russo, G.; Di Lauro, N.; Checchia, P.; Marianecci, C.; Carafa, M.; Santucci, E.; Ortaggi, G. Physicochemical and biological study of selected hydrophobic polyethylenimine-based polycationic liposomes and their complexes with DNA. *Bioorg. Med. Chem.* **2007**, *15* (3), 1504−1515.
(34) Yamazaki, Y.; Nango, M.; Matsuura, M.; Hasegawa, Y.; Hasegawa, M.; Oku, N. Polycation liposomes, a novel nonviral gene transfer system, constructed from cetylated polyethylenimine. *Gene Ther.* **2000**, *7* (13), 1148−1155.
(35) Li, J.; Zhu, Y.; Hazeldine, S. T.; Li, C.; Oupicky, D. Dual-function CXCR4 antagonist polyplexes to deliver gene therapy and inhibit cancer cell invasion. *Angew. Chem., Int. Ed.* **2012**, *51* (35), 8740−8743.
(36) Wang, Y.; Hazeldine, S. T.; Li, J.; Oupicky, D. Development of Functional Poly(amido amine) CXCR4 Antagonists with the Ability to Mobilize Leukocytes and Deliver Nucleic Acids. *Adv. Healthcare Mater.* **2015**, *4* (5), 729−738.
(37) Wang, Y.; Kumar, S.; Rachagani, S.; Sajja, B. R.; Xie, Y.; Hang, Y.; Jain, M.; Li, J.; Boska, M. D.; Batra, S. K.; Oupicky, D. Polyplex-mediated inhibition of chemokine receptor CXCR4 and chromatin-remodeling enzyme NCOA3 impedes pancreatic cancer progression and metastasis. *Biomaterials* **2016**, *101*, 108−120.
(38) Xie, Y.; Wehrkamp, C. J.; Li, J.; Wang, Y.; Wang, Y.; Mott, J. L.; Oupicky, D. Delivery of miR-200c Mimic with Poly(amido amine) CXCR4 Antagonists for Combined Inhibition of Cholangiocarcinoma Cell Invasiveness. *Mol. Pharmaceutics* **2016**, *13* (3), 1073−1080.
(39) Li, J.; Oupicky, D. Effect of biodegradability on CXCR4 antagonism, transfection efficacy and antimetastatic activity of polymeric Plerixafor. *Biomaterials* **2014**, *35* (21), 5572−5579.
(40) Abdallah, B.; Hassan, A.; Benoist, C.; Goula, D.; Behr, J. P.; Demeneix, B. A. A powerful nonviral vector for in vivo gene transfer into the adult mammalian brain: polyethylenimine. *Hum. Gene Ther.* **1996**, *7* (16), 1947−1954.
(41) Fischer, D.; Bieber, T.; Li, Y.; Elsässer, H.-P.; Kissel, T. A novel non-viral vector for DNA delivery based on low molecular weight, branched polyethylenimine: effect of molecular weight on transfection efficiency and cytotoxicity. *Pharm. Res.* **1999**, *16* (8), 1273−1279.
(42) Godbey, W.; Wu, K. K.; Mikos, A. G. Size matters: molecular weight affects the efficiency of poly (ethyleneimine) as a gene delivery vehicle. *J. Biomed. Mater. Res.* **1999**, *45* (3), 268−275.
(43) Werth, S.; Urban-Klein, B.; Dai, L.; Höbel, S.; Grzelinski, M.; Bakowsky, U.; Czubayko, F.; Aigner, A. A low molecular weight fraction of polyethylenimine (PEI) displays increased transfection efficiency of DNA and siRNA in fresh or lyophilized complexes. *J. Controlled Release* **2006**, *112* (2), 257−270.
(44) Fischer, D.; Li, Y.; Ahlemeyer, B.; Krieglstein, J.; Kissel, T. In vitro cytotoxicity testing of polycations: influence of polymer structure on cell viability and hemolysis. *Biomaterials* **2003**, *24* (7), 1121−1131.
(45) Hong, S.; Leroueil, P. R.; Janus, E. K.; Peters, J. L.; Kober, M.-M.; Islam, M. T.; Orr, B. G.; Baker, J. R., Jr; Banaszak Holl, M. M. Interaction of polycationic polymers with supported lipid bilayers and

DOI: 10.1021/acs.biomac.7b01487
Biomacromolecules XXXX, XXX, XXX−XXX

cells: nanoscale hole formation and enhanced membrane permeability. *Bioconjugate Chem.* **2006**, *17* (3), 728−734.
(46) Chen, J.; Hessler, J. A.; Putchakayala, K.; Panama, B. K.; Khan, D. P.; Hong, S.; Mullen, D. G.; Dimaggio, S. C.; Som, A.; Tew, G. N.; Lopatin, A. N.; Baker, J. R.; Holl, M. M.; Orr, B. G. Cationic nanoparticles induce nanoscale disruption in living cell plasma membranes. *J. Phys. Chem. B* **2009**, *113* (32), 11179−11185.
(47) Zhang, C.; Wu, F.-G.; Hu, P.; Chen, Z. Interaction of Polyethylenimine with Model Cell Membranes Studied by Linear and Nonlinear Spectroscopic Techniques. *J. Phys. Chem. C* **2014**, *118* (23), 12195−12205.
(48) Hancock, R. D.; Motekaitis, R. J.; Mashishi, J.; Cukrowski, I.; Reibenspies, J. H.; Martell, A. E. The unusual protonation constants of cyclam. A potentiometric, crystallographic and molecular mechanics study. *J. Chem. Soc., Perkin Trans. 2* **1996**, No. 9, 1925−1929.
(49) Luker, K. E.; Luker, G. D. Functions of CXCL12 and CXCR4 in breast cancer. *Cancer Lett.* **2006**, *238* (1), 30−41.
(50) Chatterjee, S.; Behnam Azad, B.; Nimmagadda, S. The intricate role of CXCR4 in cancer. *Adv. Cancer Res.* **2014**, *124*, 31−82.
(51) Muller, A.; Homey, B.; Soto, H.; Ge, N.; Catron, D.; Buchanan, M. E.; McClanahan, T.; Murphy, E.; Yuan, W.; Wagner, S. N.; Barrera, J. L.; Mohar, A.; Verastegui, E.; Zlotnik, A. Involvement of chemokine receptors in breast cancer metastasis. *Nature* **2001**, *410* (6824), 50−56.

DOI: 10.1021/acs.biomac.7b01487
Biomacromolecules XXXX, XXX, XXX−XXX